Journal of Fluorescence (2019) 29:865–875
https://doi.org/10.1007/s10895-019-02397-x

ORIGINAL ARTICLE

Heteroleptic Zn(II) Complexes: Synthesis, Characterization and Photoluminescence Properties

Jaydip Solanki [1] · Kiran Surati [1]

Received: 23 March 2019 / Accepted: 28 May 2019 / Published online: 20 July 2019

Abstract

Heteroleptic Zn (II) complexes containing 8-hydroxy quinoline as preliminary ligand and pyrazolone based derivatives as secondary ligand were synthesized and their structures confirmed by NMR, Mass, FT-IR, UV-vis and Elemental analysis. Theses complexes show good photoluminescence properties in solid and solution state in the range of 505–544 nm with quantum yield 0.38 to 0.50. Whereas these complexes also show good life time in the range of 0.037 to 0.043 ms. These complexes show shift in the range of 25–30 nm. in different polar and nonpolar solvents due to intramolecular charge transfer (ICT). The bandgap of these complexes is around ~2.60 eV. Highest occupied molecular orbital (HOMO) and lowest unoccupied molecular orbital (LUMO) of all complexes are determine by cyclic voltammetry it obtained in the range of and ~ (5.29 eV) and ~(2.69 eV). The energy band gap, frontier molecular orbitals (FMO) energy levels and geometrical structures were optimized using density functional theory (DFT) with B3LYP/6-31G* basic set on Spartan'18 software. All complexes displayed high thermal stability.

Keywords Luminescence · Heteroleptic Zn(II) complexes · Solvent effect

Introduction

Since the past two-three decades, the field of Organic Light Emitting Diodes (OLEDs) has shown tremendous growth due to their potential applications in low cost, more efficient flat-panel displays and solid-state lighting [1]. Generally, these devices are fabricated by using organic, inorganic molecules or organic polymers as hole transport layers, electron transport layers, dopants and hosts [2–8]. Particularly, Iridium(III), Platinum(II), Aluminum(III), Zinc(II) complexes are seen their attractive electroluminescence properties on the basis of an introductory study by C. W. Tang and S. A. Van Slyke [9–13]. Among these, zinc complexes are promising candidates in comparison to other metal because of zinc complex having some superior features like good emission, less toxicity, low molecular weight, high thermal stability, easy color tunability with simple synthesis procedure and higher reaction yields [14–17]. Metal complexes of 8-hydroxyquinoline (Mqn) and its derivatives like tris(8-hydroxyquinoline) aluminum (Alq3) and bis(8-hydroxyquinoline) zinc (Znq2) broadly considered to be one of the most credible electron transporting and emitting materials, but Znq2 exhibit higher quantum yield and improve injection efficiency than Alq3 [18–22]. The maximum OLED light output obtained when the excitons generate due to the conjunction of an electron-hole at the interface of emitting layer [23]. This circumstance is accomplished by the distribution of the electron donor (D) and electron acceptor (A) environment or both are connected with a suitable spacer [24–27]. Generally, the donor-acceptor (D-A) and donor-bridge-acceptor (D-B-A) systems of organic and inorganic molecules are used for controllable tuning the emission color and bandgap, the formation of π-conjugation charge and expeditious charge transfer from donor to acceptor [28, 29]. In view of these photophysical and electrochemical properties are essential for developing a highly competent donor-acceptor category for OLED application. The emission properties of the metal complex will be regulated by variation the ligands or by substitution the electron withdrawing and donating group in the ligands. Some research articles are available in the literature, where the replacement of electron withdrawing atoms at 2 or 5 or 5,7 positions exhibited a hypsochromic shift in the emission spectra as related to unsubstituted zincquinolate complex [30–35].

✉ Kiran Surati
kiransurati@yahoo.co.in

[1] Department of Chemistry, Sardar Patel University, Vallabh Vidyanagar, Anand, Gujarat 388120, India

In the present work mainly focus on photophysical and electrochemical properties of the synthesized heteroleptic or ternary zinc complexes by using 5,7 dihalogen (Br and Cl) substituted 8-hydroxyquinoline as primary ligand and β-diketonate ligand (5-hydroxy-3-methyl-1-phenyl-1H-pyrazole-4-carbaldehyde) as a secondary ligand. In this complexes, disubstituted 8-hydroxyquinoline behave as an electron donor (D) ligand, β-diketonate ligand behave as an electron acceptor (A) ligand and both ligands linking with bridge of zinc(II) metal ion [36, 37]. The complexes [(4-formyl-3-methyl-1-phenyl-1H-pyrazol-5-yl) oxy) (5,7-dibromo-quinolin-8-yl) oxy) zinc(II)] and [(4-formyl-3-methyl-1-phenyl-1H-pyrazol-5-yl)oxy)(5,7-dichloro-quinolin-8-yloxy)zinc(II)] are exhibited high thermal stability, effective photo-luminescence performance in solid as well as different solvents with a higher quantum yield.

Experimental Section

Materials and Measurement

1-Phenyl-3-methyl-2-pyrazoline-5-one purchase from Sigma-Aldrich. 5,7-dibromo-8-hydroxyquinoline (DBHQ) and 5,7-dichloro-8-hydroxyquinoline (DCHQ) were purchase from TCI. Zinc acetate dihydrate used was of analytical grade.

The ^{1}H NMR and ^{13}C NMR spectra were recorded using Bruker 400 MHz spectrometer with tetramethylsilane as internal standard and deuterated dimethyl sulfoxide (DMSO-d^{6}) used as a solvent. The Fourier transforms infrared spectroscopy (FT-IR) spectra were recorded on MB-3000 infra-red spectrophotometer in the range of 4000–400 cm^{-1}. The UV-Visible absorption spectra of complexes was performed using a Shimadzu 160A spectrophotometer. Mass spectra were obtained by Shimadzu LCMS-2010 spectrometer and cyclic voltammetry was recorded on CHI660E electrochemical workstation. Both differential scanning calorimetry (DSC) and thermogravimetry analysis (TGA) were done by using a Perkin Elmer Pyris 1 instrument at a heating rate of 10 °C/min under a nitrogen atmosphere. Photoluminescence(PL) spectra, quantum yield and life time study were measured by a Perkin Elmer LS-55 fluorescence spectrometer.

Synthesis

Synthesis of Ligand (L)

The ligand 5-hydroxy-3-methyl-1-phenyl-1H-pyrazole-4-carbaldehyde **(L)** was prepared by our previously reports [38].

General Procedure for the Synthesis of Zinc Complex

The complexes were synthesized by DBHQ (0.303 g, 1 mmol) or DCHQ (0.214 g, 1 mmol) and secondary ligand (L) (0.202 g, 1 mmol) in absolute ethanol at 70 °C followed by dropwise addition of zinc acetate dihydrate (0.219 g, 1 mmol) in 10 ml of same solvent at 70 °C with continuous stirring and pale yellow colored precipitates were obtained. Wash with deionized water to remove excess metal ions and then wash with absolute ethanol followed by diethyl ether and dried it.

Complex 1; [Zn(DBHQ)(L)]; [(4-Formyl-3-Methyl-1-Phenyl-1H-Pyrazol-5-Yl)Oxy) (5,7-Dibromo-Quinolin-8-Yloxy)Zinc(II)]

(Yield: 61%) Anal. calcd for $C_{20}H_{13}Br_2N_3O_3Zn$; C 50.09, H 2.73, N 8.76; Found: C 50.22, H 2.87, N 8.89; ^{1}H NMR: δ(ppm) 9.04(1H, s), 8.65(1H, d),8.49–8.41(1H, m), 7.98(2H, d), 7.77–7.69(2H, m), 7.41(2H, t), 7.18(1H, t), 2.24(3H, s); ^{13}C NMR (APT): δ(ppm) 165.12, 160.26, 146.31, 140.47, 139.49, 137.83, 135.16, 129.14, 127.81, 123.62, 119.93, 105.80, 98.10, 12.78; FT-IR (cm^{-1}): 2923, 1643, 1535, 1488, 1330, 1234, 1110, 1083, 817, 748, 686,586.

Complex 2; [Zn(DCHQ)(L)]; [(4-Formyl-3-Methyl-1-Phenyl-1H-Pyrazol-5-Yl)Oxy) (5,7-Dichloro-Quinolin-8-Yloxy)Zinc(II)]

(Yield: 68%) Anal. calcd for $C_{20}H_{13}Cl_2N_3O_3Zn$: C 42.25, H 2.30, N 7.39; Found: C 42.32, H 2.39, N 7.51; ^{1}H NMR: δ(ppm) 9.04(1H, s), 8.67(1H, d), 8.56–8.50(1H, m), 7.97(2H, d), 7.76–7.67(2H, m),7.40(2H, t), 7.16(1H, t),2.24(3H, s); ^{13}C NMR (APT): δ(ppm) 165.33, 158.69, 150.15, 146.37, 140.47, 139.48, 135.46, 129.90, 129.13, 126.18, 124.63, 123.18, 119.36, 115.21, 108.85, 106.07, 12.78; FT-IR(cm^{-1}) 2931, 1650, 1542,1458,1450, 1373, 1218, 1118, 1095, 810,748, 671, 578.

Theoretical Calculation

In additionally to understand the different photophysical properties of zinc(II) complexes 1 and 2 like the HOMO, LUMO and energy band gap, frontier molecular orbitals (FMO) energy levels and geometrical structures were optimized using density functional theory (DFT) with B3LYP/6-31G* basic set on Spartan'18 software. The optimized 3D structure with minimal energy are shown in Fig. 1 and both complexes show tetrahedral geometry.

The FMOs of both complexes are shown in Fig. 2. In the complexes, the FMOs are dominated by the molecular orbitals arising from the ligands and the Zn2+ ions are appeared to be small contribution in FMO. The HOMO and LUMO of

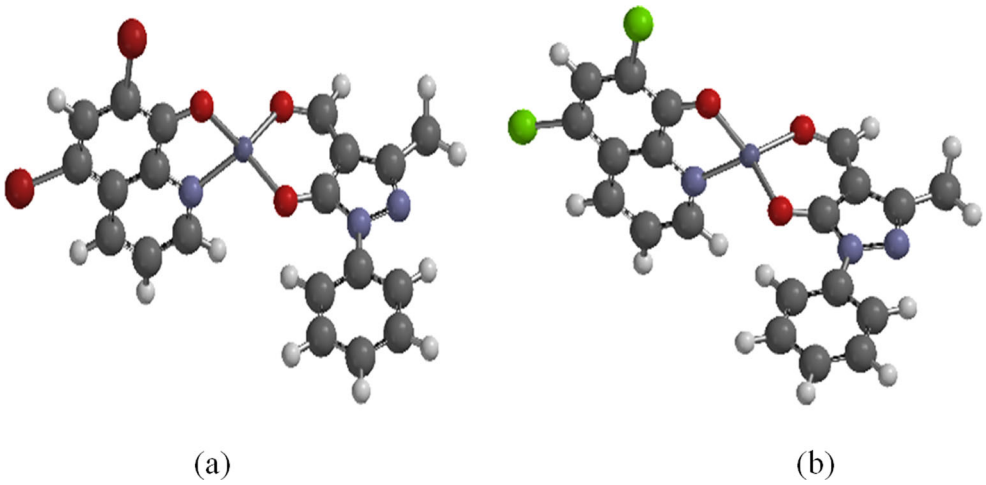

Fig. 1 3D Optimized Structure with minimal energy of **a** complex-1 and **b** complex-2

complexes are particularly localized on phenoxide and pyridyl ring of primary ligand as DBHQ and DCHQ and HOMO-1 and LUMO+1 are on secondary ligand (L). The calculated HOMO energy levels of complex 1 and 2 are −5.58 and − 5.55 eV and the LUMO energy levels are −2.25 and − 2.23 eV, respectively. So, the band gap of complex 1 and 2 are 3.33 and 3.32 eV, as per theoretical study of complexes we can be concluded that substitution of halogen on primary ligand was negligible effect and further preliminary ligand (DBHQ and DCHQ) stabilized the HOMO and LUMO and β-diketone as secondary ligand taking part to stabilized the HOMO (−1) and LUMO (+1) of complexes [34, 35].

Results and Discussion

All ligands and complexes were stable at atmospheric temperature and pressure. They were soluble in common organic solvents and characterized by spectroscopic methods, the results were good agreement with proposed structure as shown in scheme 1. The photophysical and electrochemical characteristic measurement by luminescence spectra, UV-visible spectra and cyclic voltammetry respectively. Thermal stability was measured by TGA and DSC. Theoretical calculations performed to estimate FMOs and optimized structure.

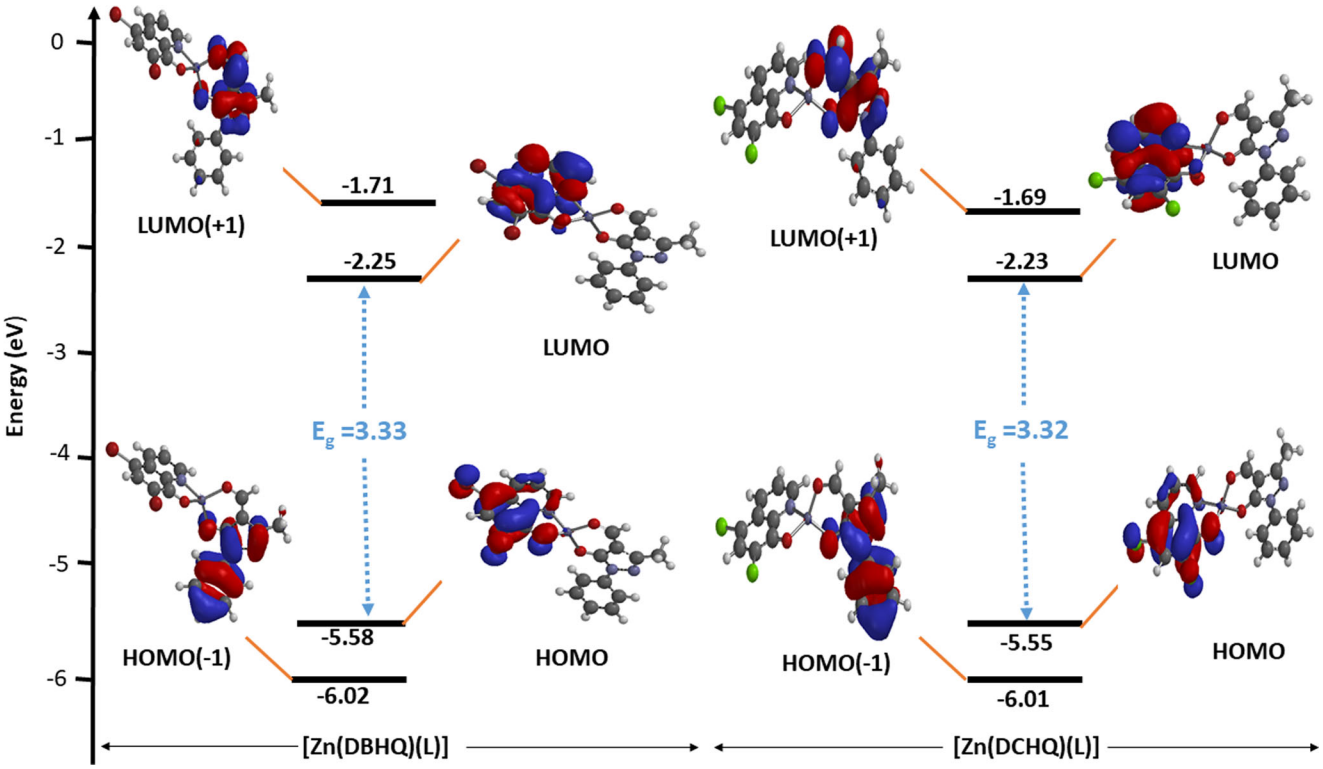

Fig. 2 Frontier molecular orbitals (FMOs) of the complexes calculated using B3LYP/6-31G*

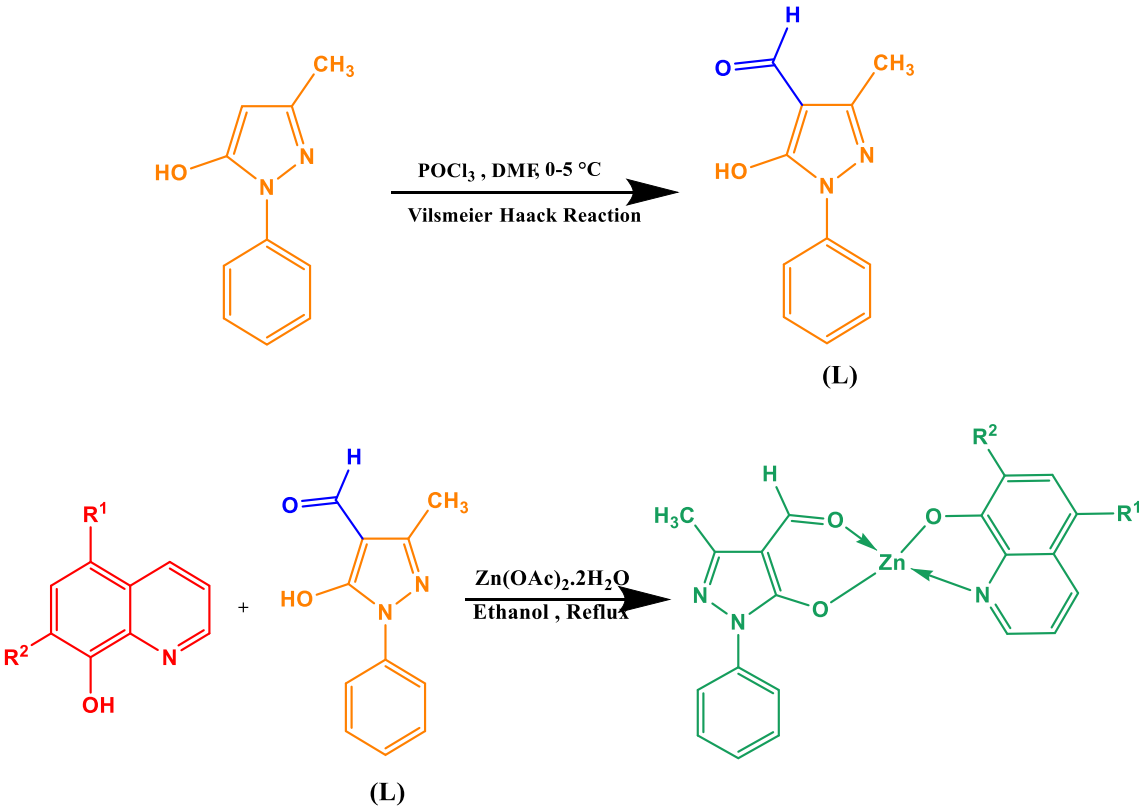

Where,

Complex 1: R^1=R^2= Br; **[Zn(DBHQ)(L)] and**

Complex 2: R^1=R^2= Cl**; [Zn(DCHQ)(L)]**

Scheme 1 Synthesis scheme of ligand and complexes. Where, Complex 1: $R^1 = R^2 = Br$; [Zn(DBHQ)(L)] and Complex 2: $R^1 = R^2 = Cl$; [Zn(DCHQ)(L)]

Complex Characterization

The synthesis scheme of Zn(II) complex was shown in scheme 1. The complexes were characterized by nuclear magnetic resonance spectroscopy (like ^{1}H NMR and ^{13}C NMR), Elemental analysis and FTIR. In ^{1}H NMR, ligands are shown the peak of enolic proton at δ 11.561 in case of secondary ligand and the singlet peak due to the hydroxyl proton at δ 9.26 in case of DBHQ and

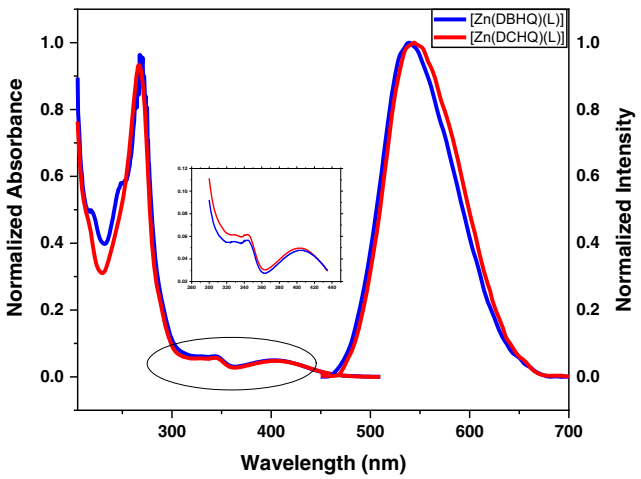

Fig. 3 Absorption and Photoluminescence Spectra of [Zn(DBHQ)(L)] and [Zn(DCHQ)(L)] measured in acetonitrile solvent

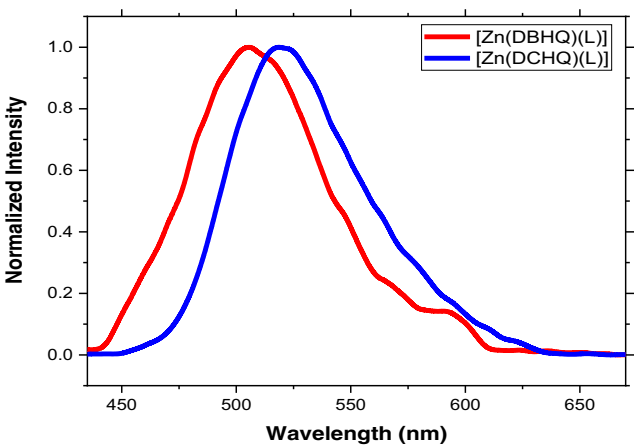

Fig. 4 Photoluminescence spectra of both complex in solid state

Table 1 UV-vis absorption, photoluminescence (PL), relative PL quantum yield and lifetime studies data of zinc complex

Complex	UV-vis absorbance (nm)	Photoluminescence (PL)						
		DMF Solution			Solid state			Lifetime (ms)
		PL λ_{max} (nm)	QY	CIE (x, y)	PL λ_{max} (nm)	QY	CIE (x, y)	
[Zn(DBHQ)(L)]	268,342,405	539	0.46	(0.36,0.58)	505	0.38	(0.19,0.48)	0.037
[Zn(DCHQ)(L)]	266,344,405	544	0.50	(0.38,0.57)	520	0.41	(0.25,0.61)	0.043

Absorption spectra measured in acetonitrile (1.0 × 10–4 M)

DCHQ, both signal disappear after complexation with Zn(II) ion, it indicates that both the enolic and hydroxyl proton takes part in complex formation. From the FT-IR spectra, the peak between 2920 and 2930 cm^{-1} indicate the stretching vibration of C-H bond in aromatic system. Other peak at 1542 and 1373 cm^{-1} which were related to the $\upsilon_{(C=N)}$ bond of the pyrazolone ring and the $\upsilon_{(C-O)}$ bond, respectively. The observed peaks in the region from 800 to 600 cm^{-1} have been shown the presence of quinoline ring. The metal sensitive stretching vibrational band at 578 cm^{-1} for both complexes can be related to the $\upsilon_{(Zn-O)}$ vibration [39].

Photophysical Properties

The Photophysical properties of complex 1 and 2 in dimethylformamide (DMF) (1.0×10^{-4} M) solution were measured by UV-vis absorption and photoluminescence spectroscopy (in Fig. 3). The acquired data are summarized in Table 1. Both complex display a multiple UV-absorption peak in the range of 230–350 nm, which are emanate from ligands centered π-π* and n-π* electronic transition and one distinct weaker band at 400–410 nm assigned as intramolecular interaction between metal-ligand charge transfer within the whole complex [40]. The energy band gap of both complex was

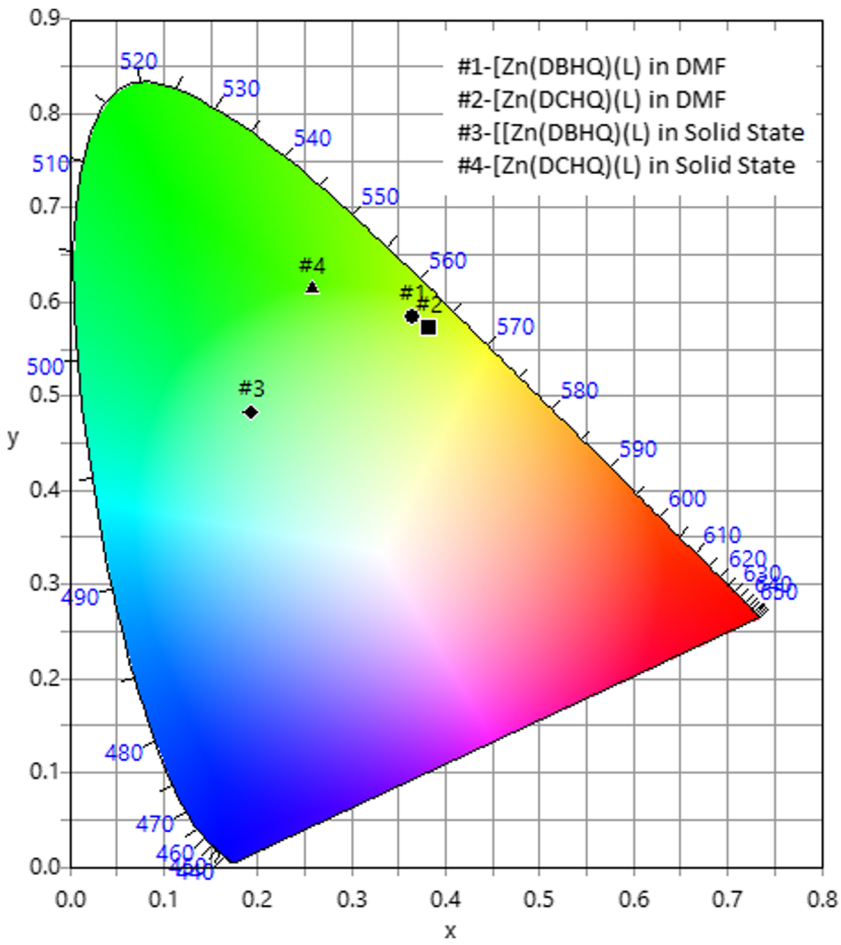

Fig. 5 CIE coordinate of both complexes in solution and solid state

estimated by Eq. 1 and calculated value are shown in Table 3.

$$\text{Band gap, Eg} = \text{hc}/\lambda_{\text{onset(UV–vis)}} \quad (1)$$

The both complex showed good luminescence properties in solution and solid states. The emission spectra of synthesized complexes were measured in DMF at room temperature, the values are 539 nm with CIE coordinate (0.36,0.58) and 544 nm with CIE coordinate (0.38,0.57) for 1 and 2 respectively (see Fig. 5). In solid state, complex 1 and 2 are exhibited strong luminescence broad band at 505 nm and 520 nm, respectively. (see Fig. 4), where Znq_2 showed emission at 560 and 496 nm in solution and solid state respectively [41].

The photoluminescence quantum yield of both complexes were measured in solution of complexes by a relative method using the reference standard in the same solvent [42]. The quantum yields were calculated by using Eq. 2 [43],

$$\textit{Quantum Yield } \Phi(x) = \Phi(r) * \frac{Abs(r)}{Abs(x)} * \frac{Area(x)}{Area(r)} * \frac{\eta 2(x)}{\eta 2(r)} \quad (2)$$

Where, $\Phi(r)$ and $\Phi(x)$ are the quantum yields of reference standard and unknown sample, $Abs(r)$ and $Abs(x)$ are the solution absorbance, $Area(r)$ and $Area(x)$ are area of the entire emission, $\eta(r)$ and $\eta(x)$ are the refractive index of the solvent.

Complex 1 and 2 are shown luminescence quantum yield (Φ) 0.46 and 0.50 which is greater than of Znq_2 (0.30) in acetonitrile, while 0.38 and 0.41 are Φ of both complexes in the solid state and it was also close to literature value of Znq_2 (0.50) [41].

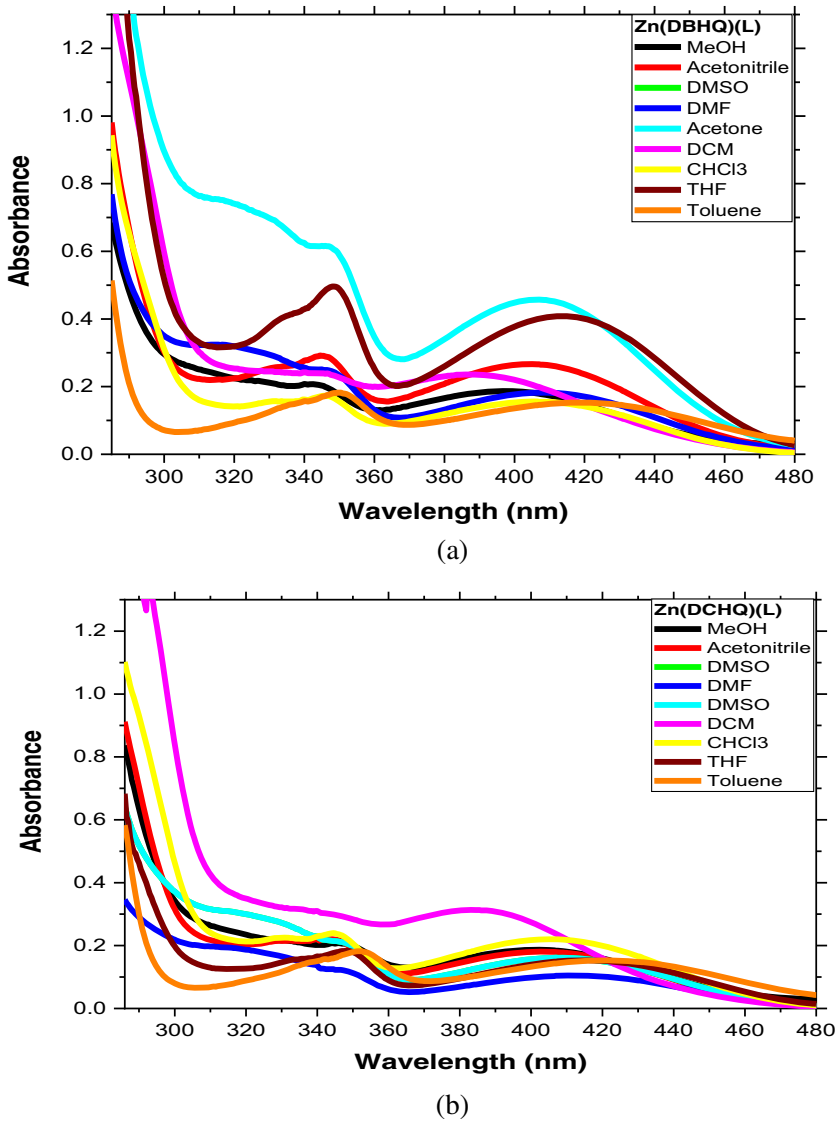

Fig. 6 Absorption spectra of **a** [Zn(DBHQ)(L)] and **b** [Zn(DCHQ)(L)] in different solvents

Solvent Effect on Absorption and Photoluminescence Spectra and its Correlation of Solvatochromic Shift with Solvent Polarity

In π-conjugated molecules with donor-acceptor (D-A) or donor-bridge-acceptor (D-B-A) type systems have been introduced intramolecular charge-transfer (ICT) character [44–46]. Such ICT character of complexes were studied by measuring the absorption and photoluminescence spectra with different polarity of solvents [47–51]. So, solvent effect of complexes studied by the absorption and photoluminescence (PL) spectra of both complexes in different solvents (Figs. 6 and 7). The absorption and luminescence spectra of both complexes recorded in different solvents with λ_{abs} and λ_{PL} obtained in range of 384–420 nm and 522–550 nm. respectively. The absorption and PL peaks values of both complexes in different solvents are summarized in Table 2. In absorption and PL spectra of both complexes blue shift on increasing polarity of solvents but in the case of acetone or DMF give red shift compered to Methanol [52–54]. Further, the liner correlation of Stoke shift (Δυ) and orientation polarizability (Δf) is obtained Lippert-Mataga plot [55–57]. The value of stoke shift and Δf of both complexes are summarized in Table 3 and Lippert-Mataga plot of both complexes are shown in Fig. 8.

Electrochemical Analysis

The electrochemical properties of synthesized zinc com plexes containing disubstituted 8-hydroxyquinoline and β-diketonate ligand were studied by cyclic voltammetry (CV). The CV experiment was performed on a CHI660E electrochemical workstation using a three assembly consist of a Platinum (Pt) disk as working electrode, a non-aqueous Ag/Ag + as a reference electrode and a subsidiary Pt electrode. Figure 9 shows the cyclic voltammograms of zinc complex 1 and 2, It was obtained by using DMF containing 0.1 M tetrabutylammonium perchlorate (TBAP) as a supporting electrolyte as well as ferrocene (Fc) as an internal standard in the potential range of −1.2 to +0.68 V for complex 1 and − 0.8 to +0.8 V for complex 2 at scan rate of 50 mV s^{-1}. The

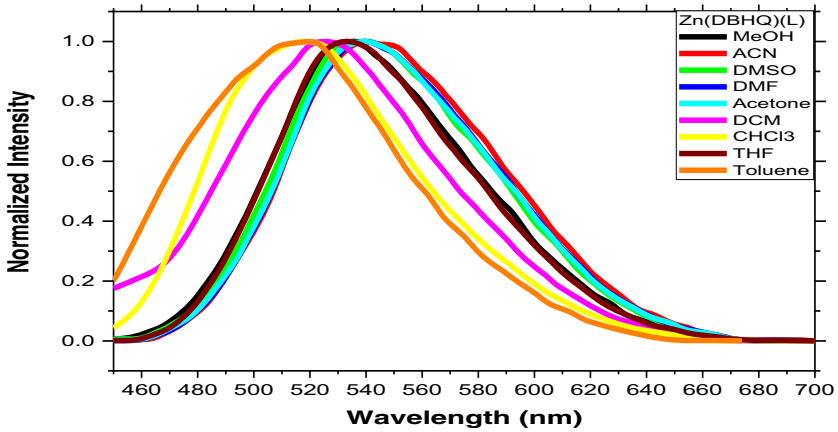

Fig. 7 PL emission spectra of **a** [Zn(DBHQ)(L)] and **b** [Zn(DCHQ)(L)] in different solvents at same excitation (400 nm)

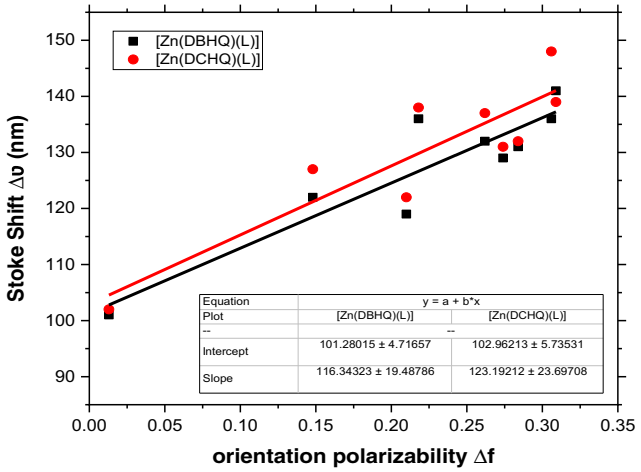

Fig. 8 Lippert-Mataga Plot of both complexes

specified electrochemical properties of both zinc complexes are summarized in Table 4.

The highest occupied molecular orbital (HOMO) and lowest unoccupied molecular orbital (LUMO) energy levels of both complexes were evaluated using Eqs. 3 and 4 [58],

$$E_{HOMO} = -\left(E_{onset(Fc+/Fc)} + 5.1\right)\ eV \quad (3)$$

$$E_{LUMO} = \left(E_{HOMO} + E_g\right)\ eV \quad (4)$$

The HOMO energy levels of complexes 1 and 2 were calculated to be −5.213 and − 5.299 eV from the onset oxidation potential, assuming the absolute energy level of ferrocenium/ferrocene (Fc+/Fc) redox couple to be 5.10 eV below the vacuum energy level [59]. The LUMO energy levels of complexes 1 and 2 were estimated to be −2.523 and − 2.699 eV, achieved from its HOMO energy level and optical band gap (calculated from its absorption λ_{onset} using Eq. 1). Therefore, the complexes are shown the difference in HOMO level of 0.086 eV and LUMO level of 0.176 eV may due to the effect

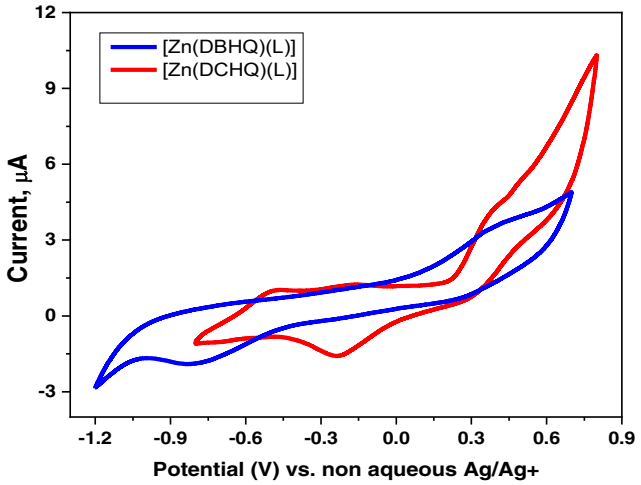

Fig. 9 Cyclic Voltammograms of [Zn(DBHQ)(L)] and [Zn(DCHQ)(L)] in DMF solvent

Table 2 Spectroscopic characteristics of investigated complexes in selected solvents

Solvents	[Zn(DBHQ)(L)]		[Zn(DCHQ)(L)]	
	λ_{abs} (nm)	λ_{PL} (nm)	λ_{abs} (nm)	λ_{PL} (nm)
MeOH	394	535	398	537
CH_3CN	404	540	402	550
DMSO	407	539	407	544
DMF	410	539	413	544
Acetone	408	539	409	541
DCM	389	525	384	522
$CHCl_3$	405	527	406	533
THF	414	533	415	537
Toluene	418	519	420	522

Where, *MeOH* methanol, CH_3CN acetonitrile, *DMSO* dimethyl sulfoxide, *DMF* dimethylformamide, *DCM* dichloromethane, *$CHCl_3$* chloroform, *THF* tetrahydrofuran

of halogen substitution on 8-hydroxyquinoline ligand. The bromine atoms have higher effect on the half-point potential compare to chlorine atom in complex [60]. Therefore, dihalogen substituted 8-hydroxy quinoline and pyrazolone ligands are more favorable for tuning the bandgap for HOMO and LUMO levels of zinc complexes for OLEDs application.

Thermal Properties

A necessary property for construction of OLEDs device is the formation of morphologically stable and uniform amorphous thin films by chemical vapor deposition (CVD) method. Therefore, thermal properties and the amorphous behavior of the synthesized zinc complexes were measured by thermogravimetry (TGA) and differential scanning

Table 3 The value of orientation polarizability(Δf) of selected solvent for Lippert-Mataga Plot

Solvents	Polarity (H_2O 100)	Δf	Stoke Shift Δυ (nm)	
			[Zn(DBHQ)(L)]	[Zn(DCHQ)(L)]
MeOH	76.2	0.309	141	139
CH_3CN	46.0	0.306	136	148
DMSO	44.4	0.262	132	137
DMF	40.4	0.274	129	131
Acetone	35.5	0.284	131	132
DCM	30.9	0.218	136	138
$CHCl_3$	25.9	0.148	122	127
THF	21.0	0.210	119	122
Toluene	9.9	0.013	101	102

Where, $\Delta f = \frac{\varepsilon-1}{2\varepsilon+1} - \frac{\eta^2-1}{2\eta^2+1}$; ε = dielectric constant of solvents and η = refractive index of solvents

Table 4 Electrochemical behavior of zinc complexes 1 and 2

Complex	E_g (eV)	E_{onset} (V)	HOMO (eV)	LUMO (eV)
1	2.69	0.113	−5.213	−2.523
2	2.60	0.199	−5.299	−2.699

calorimetry (DSC) techniques. Both complexes were heated in range of 40–500 °C with heating rate 10 °C min-1. The result of TGA shows that both complexes indicates efficient thermal stability with high decomposition temperature (T_d) greater than 320 °C. Further, the higher thermal stability referred that both complexes are amorphous in nature without glass transition temperature (Tg) [61], whereas endothermic melting transition temperature (T_m) occur at 320 and 375 °C for complexes 1 and 2 respectively. In additional significance from DSC, the endothermic peak of both complexes are observed at the higher temperature, that means both complexes existence in monomeric structure and they are not form any type of dimer or oligomer [62]. Such higher value of T_d, T_m and monomeric structure at high temperature indicate that both complexes are stable, they also offer a great potential to be fabricated device by chemical vapor deposition (CVD) and vacuum thermal evaporation technology [19].

Conclusion

In summary, two heteroleptic complexes were design based on D-B-A system. These complexes structure were characterized by spectroscopy. The photophysical and luminescence properties were revels that these complexes 1 and 2 were suitable emitters with luminescence quantum yield 0.31 and 0.41 respectively as compared with Znq_2 (0.30), whereas luminescence lifetime of complex 2 obtained value 0.041 ms which is higher as compared with complex 1 value 0.037 ms. Here, ligand DCHQ in complex 2 shows higher lifetime and luminescence quantum yield due to their less non-radiative decay as compared with complex 1. Moreover, the band gap of complex 2 were also favorable 2.60 eV with other host materials. These complexes were thermally stable up to 320 °C and show endo thermic melting transition at 320 and 375 °C for complex 1 and 2 respectively. It further suitable for device processibility of these material. In conclusion, the design complexes were good emitter material with the above mention luminescence, photophysical, electrochemical and thermal properties for OLEDs application.

Acknowledgements Authors express sincere thanks to Department of Science and Technology (DST), New Delhi, for financial support under Scheme of Young Scientist & Technologist (SYST) (Ref.No.SP/YO/008/2017(G)) Authors are also thankful to the Head, Department of Chemistry, Sardar Patel University, Centre for Advance study (CAS) (No.F.540/3/CAS/2011(SAP-I) instrumental facility for providing basic infrastructural and instrumental facility, SICART, Vallabha Vidyanagar for instrumental facility. We also thankful to Prof. S. S. Soni for their support and cyclic voltammetry measurements

References

1. Baldo MA, O'Brien DF, You Y, Shoustikov A, Sibley S, Thompson ME, Forrest SR (1998) Highly efficient phosphorescent emission from organic electroluminescent devices. Nature 395:151–154
2. Friend RH, Gymer RW, Holmes AB, Burroughes JH, Marks RN, Taliani C, Bradley DDC, Santos DAD, Bredas JL, Logdlund M, Salaneck WR (1999) Electroluminescence in conjugated polymers. Nature 397:121–128
3. Sudhakar M, Djurovich PI, Hogen-Esch TE, Thompson ME (2013) Phosphorescence quenching by conjugated polymers. J Am Chem Soc 125:7793–7796
4. Bamesberger A, Schwartz C, Song Q, Han WW, Wang Z, Cao H (2014) Rational design of a rapid fluorescent approach for detection of inorganic fluoride in MeCN–H2O: a new fluorescence switch based on N-aryl-1,8-naphthalimide. New J Chem 38:884–888
5. Forrest SR (2004) The path to ubiquitous and low-cost organic electronic appliances on plastic. Nature 428:911–918
6. Jurow MJ, Mayr C, Schmidt TD, Lampe T, Djurovich PI, Brutting W, Thompson ME (2016) Understanding and predicting the orientation of heteroleptic phosphors in organic light-emitting materials. Nat Mater 15:85–91
7. Osawa M, Kawata I, Ishii R, Igawa S, Hashimoto M, Hoshino M (2013) Application of neutral d^{10} coinage metal complexes with an anionic bidentate ligand in delayed fluorescence-type organic light-emitting diodes. J Mater Chem C 1:4375–4383
8. Xu BS, Wang H, Hao YY, Gao ZX, Zhou HF (2007) Preparation and performance of a new type of blue light-emitting material δ-Alq_3. J Lumin 122-123:663–666
9. Wang R, Liu D, Ren H, Zhang T, Yin H, Liu G, Li J (2011) Highly efficient Orange and white organic light-emitting diodes based on new Orange iridium complexes. Adv Mater 23:2823–2827
10. Sojoto T, Djurovich PI, Tamayo A, Yousufuddin M, Bau R, Thompson ME, Holmes RJ, Forrest SR (2005) Blue and near-UV phosphorescence from iridium complexes with Cyclometalated Pyrazolyl or N-heterocyclic Carbene ligands. Inorg Chem 44: 7992–8003
11. Tronnier A, Heinemeyer AU, Metz S, Wagenblast G, Muensterb I, Strassner T (2015) Heteroleptic platinum(II) NHC complexes with a C^C* cyclometalated ligand – synthesis, structure and photophysics. J Mater Chem C 3:1680–1693
12. Wang JF, Jabbour GE, Mash EA, Anderson J, Zhang YD, Lee PA, Armstrong NR, Peyghambarian N, Kippelen B (1998) Oxadiazole metal complex for organic light-emitting diodes. Adv Mater 11: 1266–1269
13. Tang CW, Van Slyke SA (1987) Organic electroluminescent diodes. Appl Phys Lett 51:913–915
14. Dumur F, Beouch L, Tehfe M, Contal E, Lepeltier M, Wantz G, Graff B, Goubard F, Mayer CR, Lalevée J, Gigmes D (2014) Low-cost zinc complexes for white organic light-emitting devices. Thin Solid Films 564:351–360
15. Du N, Mei Q, Lu M (2005) Quinolinate aluminum and zinc complexes with multi-methyl methacrylate end groups: synthesis, photoluminescence, and electroluminescence characterization. Synth Met 149:193–197
16. Chen X, Qiu D, Ma L, Cheng Y, Geng Y, Xie Z, Wang L (2006) Synthesis, crystal structure, spectroscopy and electroluminescence of zinc(II) complexes containing bidentate 2-(2-pyridyl) quinoline derivative ligands. Transit Met Chem 31:639–644

17. Dumur F (2014) Zinc complexes in OLEDs: an overview. Synth Met 195:241–251
18. Xu X, Yu G, Liu Y, Tang R, Xi F, Zhu D (2005) Effect of metal chelate layer on electroluminescent and current-voltage characteristics. Appl Phys Lett 86:202109
19. Sapochak LS, Benincasa FE, Schofield RS, Baker JL, Riccio KC, Fogarty D, Kohlmann H, ferris KF, Burrows PE (2002) Electroluminescent zinc(II) Bis(8-hydroxyquinoline): structural effects on electronic states and device performance. J Am Chem Soc 124:6119–6125
20. Meyers A, South C, Weck M (2014) Design, synthesis, characterization, and fluorescent studies of the first zinc-quinolate polymer. Chem Commun 0:1176–1177
21. Hopkins TA, Meerholz K, Shaheen S, Anderson ML, Schmidt A, Kippelen B, Padias AB, Hall JHK, Peyghambarian N, Armstrong NR (1996) Substituted aluminum and zinc Quinolates with blue-shifted absorbance/luminescence bands: synthesis and spectroscopic, photoluminescence, and electroluminescence characterization. Chem Mater 8:344–351
22. Ghedini M, Deda ML, Aiello I, Grisolia A (2003) Synthesis and photophysical characterization of soluble photoluminescent metal complexes with substituted 8-hydroxyquinolines. Synth Met 138: 189–192
23. La Deda M, Grisolia A, Aiello I, Crispini A, Ghedini M, Belviso S, Amati M, Lelj F (2004) Investigations on the electronic effects of the peripheral 4′-group on 5-(4′-substituted) phenylazo-8-hydroxyquinoline ligands: zinc and aluminium complexes. Dalton Trans (16):2424–2431
24. Sandee AJ, Williams CK, Evans NR, Davies JE, Boothby CE, Koehler A, Friend RH, Holmes AB (2004) Solution-Processible conjugated Electrophosphorescent polymers. J Am Chem Soc 126:7041–7048
25. Kirk ML, Shultz DA (2013) Transition metal complexes of donor–acceptor biradicals. Coord Chem Rev 257(1):218–233
26. Xu H, Chen R, Sun Q, Lai W, Su Q, Huang W, Liu X (2014) Recent progress in metal–organic complexes for optoelectronic applications. Chem Soc Rev 43:3259–3302
27. Zhang Y, Chen Z, Wang X, He J, Wu J, Liu H, Song J, Qu J, Chan W, Wong W (2018) Achieving NIR emission for donor–acceptor type platinum(II) complexes by adjusting coordination position with isomeric ligands. Inorg Chem 57:14208–14217
28. Bauer P, Wietasch H, Lindner SM, Thelakkat M (2007) Synthesis and characterization of donor−bridge−acceptor molecule containing Tetraphenylbenzidine and Perylene Bisimide. Chem Mater 19: 88–94
29. Berlin YA, Grozema FC, Siebbeles LDA, Ratner MA (2008) Charge transfer in donor-bridge-acceptor systems: static disorder, dynamic fluctuations, and complex kinetics. J Phys Chem C 112: 10988–11000
30. Sharma A, Singh D, Makrandi JK, Kamalasanan MN, Shrivastva R, Singh I (2007) Electroluminescent characteristics of OLEDs fabricated with bis(5,7-dichloro-8-hydroxyquinolinato) zinc(II) as light emitting material. Mater Lett 61:4614–4617
31. Huo Y, Lu J, Lu T, Fang X, Ouyang X, Zhang L, Yuan G (2015) Comparative studies on OLED performances of chloro and fluoro substituted Zn(II) 8-hydroxyquinolinates. New J Chem 39:333–341
32. Pohl R, Montes VA, Shinar J, Anzenbacher P (2004) Red−green −blue emission from Tris(5-aryl-8-quinolinolate)Al(III) complexes. J Organomet Chem 69:1723–1725
33. Barberis VP, Mikroyannidis JA (2006) Synthesis and optical properties of aluminum and zinc quinolates through styryl subsituent in 2-position. Synth Met 156:865–871
34. Kumar A, Palai AK, Shrivastava R, Kadyan PS, Kamalsanan MN, Singh I (2014) N-type ternary zinc complexes: synthesis, physicochemical properties and organic light emitting diodes application. J Organomet Chem 756:38–46
35. Kumar A, Srivastava R, Kumar A, Nishal V, Kadyan PS, Kamalasanan MN, Singh I (2013) Ternary zinc complexes as electron transport and electroluminescent materials. J Organomet Chem 740:116–122
36. Lakshmi A, Balachandran V, Janaki A (2011) Comparative vibrational spectroscopic studies, HOMO–LUMO and NBO analysis of 5,7-dibromo-8-hydroxyquinoline and 5,7-dichloro-8-hydroxyquinoline based on density functional theory. J Mol Struct 1004:51–66
37. Kumar S, Surati KR, Lawrence R, Vamja AC, Yakunin S, Kovalenko MV, Santos EJG, Shih C (2017) Design and synthesis of Heteroleptic iridium(III) phosphors for efficient organic light-emitting devices. Inorg Chem 56:15304–15313
38. Surati KR, Thaker BT (2010) Synthesis, spectral, crystallography and thermal investigations of novel Schiff base complexes of manganese (III) derived from heterocyclic β-diketone with aromatic and aliphatic diamine. Spectrochim Acta Part A 75:235–242
39. Nakamoto K (1978) Infrared and Raman spectra of inorganic and coordination compounds, 3rd edn. John Wiley and Sons, New York, p 242
40. Gusev A, Shul'gin V, Braga E, Zamnius E, Starova G, Lyssenko K, Eremenko I, Linert W (2018) Luminescent properties of zinc complexes of 4-formylpyrazolone based azomethine ligands: excitation-dependent emission in solution. J Lumin 202:370–376
41. Tsuboi T, Naka Y, Torii Y (2012) Photoluminescence of bis(8-hydroxyquinoline) zinc (Znq_2) and magnesium (Mgq_2). Cent Eur J Phys 10:524–528
42. Melhuish WH (1961) Quantum efficiencies of fluorescence of organic substances: effect of solvent and concentration of the fluorescent solute. J Phys Chem 65:229–235
43. Brouwer A (2011) Standards for photoluminescence quantum yield measurements in solution (IUPAC technical report). Pure Appl Chem 83:2213–2228. https://doi.org/10.1351/PAC-REP-10-09-31
44. Jenekhe SA, Lu L, Alam MM (2001) New conjugated polymers with donor−acceptor architectures: synthesis and Photophysics of Carbazole−Quinoline and phenothiazine−Quinoline copolymers and oligomers exhibiting large intramolecular charge transfer. Macromolecules 34:7315–7324
45. Chen R, Zhao G, Yang X, Jiang X, Liu J, Tian H, Gao Y, Liu X, Han K, Sun M, Sun L (2008) Photoinduced intramolecular charge-transfer state in thiophene-π-conjugated donor–acceptor molecules. J Mol Struct 876:102–109
46. Pappenfus TM, Schneiderman DK, Casado J, López Navarrete JT, Delgado MCR, Zotti G, Vercelli B, Lovander MD, Hinkle LM, Bohnsack JN, Mann KR (2011) Oligothiophene Tetracyanobutadienes: alternative donor−acceptor architectures for molecular and polymeric materials. Chem Mater 23:823–831
47. Reichardt C (1994) Solvatochromic dyes as solvent polarity indicators. Chem Rev 94:2319–2358
48. Acar N, Kurzawa J, Fritz N, Stockmann A, Roman C, Schneider S, Clark T (2003) Phenothiazine−pyrene dyads: Photoinduced charge separation and structural relaxation in the CT state. J Phys Chem A 107:9530–9541
49. Yang J-S, Liau K-L, Wang C-M, Hwang C-Y (2004) Substituent-dependent Photoinduced intramolecular charge transfer in N-aryl-substituted trans-4-Aminostilbenes. J Am Chem Soc 126(36): 12325–12335
50. Homocianu M, Airinei A, Dorohoi DO (2011) Solvent effects on the electronic absorption and fluorescence spectra. J Adv Res Phys 2:011105
51. Desai VR, Hunagund SM, Basanagouda M, Kadadevarmath JS, Sidarai AH (2016) Solvent effects on the electronic absorption and fluorescence spectra of HNP: Estimation of ground and excited state dipole moments. J Fluoresc 26:1391–1400
52. Zhang J, Zhao C, Liu H, Lv Y, Liu R, Zhang S, Chen H, Zhang G, Tian Z (2015) Solvatochromic fluorescence emission of an Anthranol

derivative without typical donor–acceptor structure: an experimental and theoretical study. J Phys Chem C 119(5):2761–2769
53. Rauf MA, Hisaindee S, Graham JP, Nawaz M (2012) Solvent effects on the absorption and fluorescence spectra of cu(II)-phthalocyanine and DFT calculations. J Mol Liq 168:102–109
54. Pawlowska Z, Lietard A, Aloi¨se S, Sliwa M, Idrissi A, Poizat O, Buntinx G, Delbaere S, Perrier A, Maurel F, Jacques P, Abe J (2011) The excited state dipole moments of betaine pyridinium investigated by an innovative solvatochromic analysis and TDDFT calculations. Phys Chem Chem Phys 13:13185–13195
55. Lippert E (1955) Dipolmoment und Elektronenstruktur von angeregten Molekülen. Z Naturforsch 10a:541–545
56. Noboru M, Yozo K, Masao K (1956) Solvent effects upon fluorescence spectra and the Dipolemoments of excited molecules. Bull Chem Soc Jpn 29:465–470
57. J. R. Lakowicz (2006) Principles of fluorescence spectroscopy. Springer, ISBN 0-387-31278-1. https://doi.org/10.1007/978-0-387-46312-4
58. Leonat L, Sbarcea G, Branzoi IV (2013) Cyclic voltammetry for energy levels estimation of organic materials. UPB Sci Bull Series B 75(3):111–118
59. C. Wang (2017) Electronic structure of π-conjugated materials and their effect on organic photovoltaics ISBN: 978-91-7685-393-1 pp 31-33
60. Chuang C, Santos O, Xu X, Canary JW (1997) Synthesis and cyclic voltammetry studies of copper complexes of Bromo- and Alkoxyphenyl-substituted derivatives of Tris(2-pyridylmethyl)amine: influence of cation−Alkoxy interactions on copper redox potentials. Inorg Chem 36:1967–1972
61. Perera L (2012) Organic light emitting diodes - the use of rare-earth and transition metals. Pan Standford Publisher, Singapore
62. Haines PJ (1995) Thermal method of analysis principle, application and problems. Blackie Academic & Professional Publisher, London